Journal of Petroleum Science and Engineering, 7 (1992) 91–103
Elsevier Science Publishers B.V., Amsterdam

Relative permeability hysteresis in micellar flooding

Eli Eikje[a,1], Stein R. Jakobsen[a,2], Arild Lohne[a] and Svein M. Skjæveland[b]
[a]*Rogaland Research Institute, P.O. Box 2503 Ullandhaug, N-4004 Stavanger, Norway*
[b]*Rogaland University Center, P.O. Box 2557 Ullandhaug, N-4004 Stavanger, Norway*

(Received March 15, 1991; revision accepted October 23, 1991)

ABSTRACT

Eikje, E., Jakobsen, S.R., Lohne, A. and Skjæveland, S.M., 1992. Relative permeability hysteresis in micellar flooding. In: O. Vikane (Editor), Enhanced Oil Recovery. *J. Pet. Sci. Eng.*, 7: 91–103.

This paper presents two-phase relative permeability curves for drainage and imbibition measured by the displacement method for (1) excess water–microemulsion, and (2) excess oil–microemulsion. The results show that the relative permeability curves are process dependent, even at the low interfacial tension of 0.1 mN/m for microemulsion–water, and 0.005 mN/m for microemulsion–oil.

Three-phase displacement experiments are interpreted by Virnovskii's theory, which is an extension of the two-phase JBN-method. The measured three-phase relative permeability curves are compared with those from Stone's method I.

A new hysteresis scheme is implemented in a chemical simulator and allows for saturation reversal at any point, with different curvatures for drainage and imbibition.

The validity of Virnovskii's theory is demonstrated, also when the relative permeabilities exhibit hysteresis.

Introduction

Fayers (1989) notes that three-phase relative permeabilities play a central role in most major reservoir simulators, including both black oil and EOR applications, for fluid flow processes like water drive with free gas present, gas displacement with multi-contact miscibility, and development of a middle phase microemulsion in a surfactant system. It is important to trace the zero oil isoperm for the different processes, since this isoperm determines the ultimate oil recovery (Fayers and Matthews, 1984).

Nearly all three-phase data reported in the literature have been measured by steady-state flow, since an interpretation method has been wanting for unsteady-state displacement experiments. Several research groups (Maini et al., 1989; Oak, 1990; Oak et al., 1990) have reported comprehensive series of three-phase, steady-state experiments, classified by three letters: e.g. DDI for Decreasing brine saturation, Decreasing oil saturation, and Increasing gas saturation. The notation may not be sufficiently precise for flow processes where hysteresis effects are pronounced.

Dria et al. (1990) summarize several of the problems with representing three-phase relative permeabilities. They find that there is no universally accepted conclusion as to the shape of the isoperms when the data are plotted on a saturation ternary, and they question if the saturation path is well defined in a steady-state measurement series.

In this paper we present experimental data to demonstrate that hysteresis effects are pres-

Correspondence to: S.M. Skjæveland, Rogaland University Center, P.O. Box 2557 Ullandhaug, N-4004 Stavanger, Norway.
[1]Present address: Saga Petroleum a.s.
[2]Present address: Restek A/S.

ent in micellar flooding, and suggest procedures for implementing the effect in reservoir simulators by a new relative permeability hysteresis scheme. Also, we have investigated the validity of Virnovskii's (1984) theory for interpreting three-phase displacement experiments, when hysteresis is present.

Three-phase flow considerations

Viscous instability

Analytical solutions for multiphase flow are restricted to one dimension: the JBN-method (Johnson et al., 1959) for two phases, and Virnovskii's (1984) method for three phases. Since laboratory experiments take place in three spatial dimensions, viscous fingers may develop and destroy the uni-dimensionality of the flood, and the results are in a strict sense not interpretable.

Peters and Khataniar (1987) define a stability number N_s for displacement of oil by water, slightly modified:

$$N_s=\frac{(M-1)\mu_w d^2}{N_w k\sigma}u \qquad (1)$$

where M is the mobility ratio, μ_w water viscosity, d core diameter, k absolute permeability, σ interfacial tension, and u Darcy velocity. The wettability constant N_w makes the expression rather impractical.

Peters and Khataniar's (1987) experiments show that the relative permeability of the displacing phase increases and that of the displaced phase decreases as N_s increases. For high values, the relative permeabilities are independent of N_s. The authors claim that to properly simulate unstable reservoir displacement, dynamic relative permeabilities should be acquired in the laboratory at the same degree of instability as in the reservoir.

Pavone (1989) suggests the stability number:

$$N_s=\frac{(\mu_o-\mu_r)^2}{\mu_r\sigma\phi}u \qquad (2)$$

for epoxy resin displacing oil. When $N_s>10^{-4}$, the displacement is unstable. Here μ_o is the oil viscosity, μ_r viscosity of resin, and ϕ the porosity.

Both Peters and Khataniar (1987) and Pavone (1989) imply that if the fronts are unstable, the relative permeability curves should still be derived by the uni-dimensional theory. This corresponds to performing a cross-sectional averaging over the viscous fingers. These relative permeabilities vary with the stability number in the intermediate range, and are constant at high values.

Relative permeability correlations

Dria et al. (1990) give a summary of the relative permeability correlations published for the middle phase. In the present work we have chosen the Stone's model I (Stone, 1970) as modified by Fayers (1984).

Hysteresis

Lake (1989) uses the terms *trapping* and *drag hysteresis*. From the measurements of Peters and Khataniar (1987) and Pavone (1989), we suggest the term *instability hysteresis* to characterize the following situation: A stable displacement generates relative permeability curves like those for steady-state flow (Peters and Khataniar, 1987). Reversing the flow direction, the relative permeabilities change in accordance with the stability number, and the sequence results in a hysteresis loop.

In general, we suggest that the shapes of the relative permeability curves and the hysteresis loops should depend on both capillary and stability number.

Procedures for incorporating multiphase-flow hysteresis in numerical models have been suggested by Killough (1976) and Carlson

(1981). Their algorithms are expansions of Land's (1968, 1971) ideas.

Carlson treats hysteresis in a non-wetting phase in a two-phase system and assumes the wetting-phase relative permeability to be reversible.

Killough considers hysteresis both in capillary pressures and relative permeabilities to wetting and non-wetting phases. For simplicity, he assumes the imbibition relative permeabilities to be reversible, yet points out that experimental evidence supports the idea of irreversibility.

For three-phase flow, Killough (1976) suggests that Stone's method (Stone, 1973) could be used with hysteretic two-phase curves. This procedure has recently been implemented in an industrial reservoir simulator (Quandalle and Sabathier, 1989), restricted to reversible imbibition curves.

If hysteresis effects had been implemented in three-phase relative permeabilities, we believe that some of their ambiguities could be removed. For instance, fig. 9 in the work of Oak (1990) displays a saturation ternary of oil isoperms for five different DDI processes. Let S denote saturation, subscript o oil, w water, and g gas. Around saturation values of $S_w=0.5$, $S_o=0.2$, $S_g=0.3$ the isoperms converge with values ranging from 0.001 to 0.02. With a proper hysteresis scheme, these variations could be accounted for.

As another example, it is difficult to conceive how one should employ a three-phase relative permeability correlation, e.g. Stone I, without a hysteresis scheme. For instance, Oak (1990) applies the Stone correlations to a DDI process. They choose water/oil drainage and gas/oil drainage curves. This choice is inconsistent, however, since the oil saturation is increasing in the first case and decreasing in the second, while in the three-phase experiment the oil saturation is decreasing.

The experimental data in this work make it is necessary to include irreversible hysteresis loops both for wetting and the non-wetting phases, as detailed in the Appendix.

Displacement experiments

Two-phase displacement experiments are routinely interpreted by the JBN-method (Johnson et al., 1959). Until recently, the only theory available for interpretation of three-phase displacement experiments was published by Sarem (1966). He assumed that each phase relative permeability only depends on it's own saturation. This limitation was removed by Grader and O'Meara (1988). Their derivation is incomplete, however, since they do not consider the formation of saturation discontinuities. Rather, they seem to imply that only post-breakthrough data may be interpreted.

In the Russian literature, a solution was presented by Virnovskii (1984). The expressions for calculating the relative permeability curves are the same as those of Grader and O'Meara (1988). Virnovskii, however, pays due attention to discontinuities in saturation profiles that may arise during the flood. The expressions are valid from the start of the experiment, during two-phase flow intervals and across discontinuities:

$$S_j(l,t)=S_j(x,0)-Q_{pj}(t)+f_j(l,t)Q_p(t) \quad (3a)$$

$$k_{rj}=\frac{f_j(l,t)\mu_j l}{k[z(l,t)-Q_p(t)\mathrm{d}z/\mathrm{d}Q_p]} \quad (3b)$$

where:

$$z=\frac{p(l,t)-p(0,t)}{u(t)} \quad (3c)$$

with phase label $j\in$[w,m,o], l length of core, t time, x distance along core; $Q_{pj}=1\phi l\int_0^t u_j(\tau)\mathrm{d}\tau$, produced pore volumes of phase j; $Q_p=1\phi l\int_0^t u(\tau)\mathrm{d}\tau$, total pore volumes of fluids produced; $f_j=u_j/u$, k_{rj} relative permeability, p pressure.

The required data are the same as for the standard JBN-method: pressure drop and pro-

duced volumes as functions of time. One, two or three phases may be injected at fixed ratios, and the total rate may vary with time.

If hysteresis is present, shocks that arise during the flood may send the system into consecutive hysteresis loops. The relative permeabilities will then depend on the saturation history, and the validity of the theory remains to be demonstrated.

Experiments

Two-phase displacement experiments were performed with microemulsion saturation, S_m, increasing and decreasing to acquire input for three-phase relative permeability correlations.

Three three-phase displacements were conducted. Two of them, Runs 7 and 8 produced little water, and are not included. In Run 9, oil and water were simultaneously injected.

Rock and fluid properties

The properties of the two Berea sandstone cores are shown in Table 1. Core I was used in all runs, except Run 9. The cores were heated at 800°C for six hours to neutralize clay minerals (Shaw et al., 1989), and to minimize surfactant adsorption.

The fluid system closely resembles that of Skauge and Matre (1991). The surfactant was SDBS (sodium dodecylbenzene sulfonate) with a molecular weight of 348.48 g/mol, SBA (sec. butanol) as co-solvent, and n-heptane as oil. A synthetic brine (Table 2) with mono- and divalent ions was employed to ensure constant phase properties during the flood.

The composition displayed three-phase behavior with a short equilibration time. The surfactant concentration is relatively high, and the composition will only be slightly affected if some adsorption should take place.

When mixing, a foam was created at the water–microemulsion interface. The foam was removed before further mixing.

Batch I and II were made with the same composition. They have slightly different volume fractions due to uncertainties in weights and temperature variations in the laboratory, as shown in Table 3. In the table are also listed the viscosities and densities of the three phases.

The interfacial tension between water and microemulsion was measured with a spinning drop interfacial tensiometer, and between oil and microemulsion it was determined from Huh's (1979) correlation (Table 4).

The capillary pressure may be estimated from measurements with other fluids in Berea cores with approximately the same properties, scaling the values by the ratio of the interfacial tensions. The associated capillary end effect is negligible since the scaling factor of Kyte and

TABLE 1

Properties of Berea cores I and II

Berea core	I	II
Diameter	3.73 cm	3.75 cm
Length	28.8 cm	29.7 cm
Porosity	0.228	0.222
Permeability	332 mD	261 mD

TABLE 2

Composition of solution

Component	Weight (%)
SDBS	5.46
Synthetic brine	43.62
n-heptane	42.24
SBA	8.68

TABLE 3

Properties of the three phases

Batch	Water	Emulsion	Oil
Volume fraction			
I	0.31	0.46	0.23
II	0.31	0.44	0.25
Viscosity (mPa s)			
I	1.39	2.74	0.48
II	1.40	2.92	0.45
Densities (g/cm³)			
I	1.0350	0.8001	0.6956
II	1.0351	0.7980	0.6945

TABLE 4

Interfacial tension of three-phase system

Interfacial tension (mN/m)		
Batch	Microemulsion/w	Microemulsion/oil
I	0.083	0.004
II	0.091	0.005

TABLE 5

Equipment used in displacement experiments

Pump	Waters HPLC Model 590
Power supply	Bang & Olufsen SN 14
Transmitter	Honeywell Smart ST 3000
Logger	YEW Hybrid Recorder 3088
PC	HP 87XM
Piston cells	RRI make
Core holder	RRI make

Rapoport (1958) is 3.7 for water and 7.2 for the microemulsion phase.

We have not determined the wetting characteristics of the fluids, but we assume that excess water is the wetting phase, oil the nonwetting phase, and microemulsion the middle phase, in agreement with Skauge and Matre (1991).

Equipment and procedures

The equipment is listed in Table 5. All experiments were performed at room temperature on a horizontal core, and at a rate of 1 ml/min. The pressure drop over the core was logged continuously, and production monitored by reading the menisci between the phases in a burette.

The core was cleaned after each run by methanol followed by nitrogen. The permeability decreased slightly for each run. Heating the core restored the original permeability within the accuracy of the measurements.

Two-phase displacements

The sequence of two-phase displacements is listed in Table 6. Runs 4–6 were performed with irreducible water present, and all runs were discontinued when essentially only the injected fluid was produced. In Table 6, d/o→m(w) denotes a drainage process where excess oil is displacing microemulsion at irreducible water saturation.

Before Run 4, the excess oil was mixed with excess water and microemulsion that already had passed through the core. Otherwise, the phase equilibrium could have shifted due to rock adsorption of surfactant and ion-exchange.

Absolute permeability measured with synthetic brine was used to normalize the relative permeabilities derived from the experimental data by the JBN-method.

Initial and endpoint saturations are also shown in Table 6. Note that the six runs were performed in sequence. The capillary number is calculated from $N_{ca}=\mu_j u/\sigma_{jk}$, where j refers to the displacing phase, k to the displaced phase.

Microemulsion–excess water

The core is initially 100% saturated with excess water. In Run 1, microemulsion broke through with high fractional flow and relative permeability values are only determined at high microemulsion saturation.

In Run 2, excess water broke through with a low fractional flow. Relative permeabilities are calculated over a significant saturation interval.

In order to prepare the core for displacement with oil, microemulsion was again injected in Run 3, to establish residual water saturation.

In Fig. 1 are plotted the relative permeabilities for the microemulsion phase, and excess water in Fig. 2. The direction of saturation change is indicated by arrows, and the purported hysteresis loops are made by curve-fitting a third order polynomial to the datapoints.

To represent the hysteresis loop in a reservoir simulator, an improved algorithm is needed. Carlson's (1981) procedure has to be

TABLE 6

Sequence of two-phase displacements. Core initially 100% saturated with excess water—d: drainage, i: imbibition

Run	Process	Initial saturations			Endpoint saturations			Endpoint rel. perm.	N_{ca}
		S_w	S_m	S_o	S_w	S_m	S_o		
1	d/m→w	1.000	0.000	0.000	0.117	0.883	0.000	0.781	5.0×10^{-4}
2	i/w→m	0.117	0.883	0.000	0.620	0.380	0.000	0.629	2.6×10^{-4}
3	d/m→w	0.620	0.380	0.000	0.169	0.831	0.000	0.583	5.0×10^{-4}
4	d/o→m(w)	0.169	0.831	0.000	0.169	0.302	0.529	0.647	1.2×10^{-3}
5	i/m→o(w)	0.169	0.302	0.529	0.169	0.824	0.007	0.570	6.7×10^{-3}
6	d/o→m(w)	0.169	0.824	0.007	0.169	0.255	0.576	0.583	1.2×10^{-3}

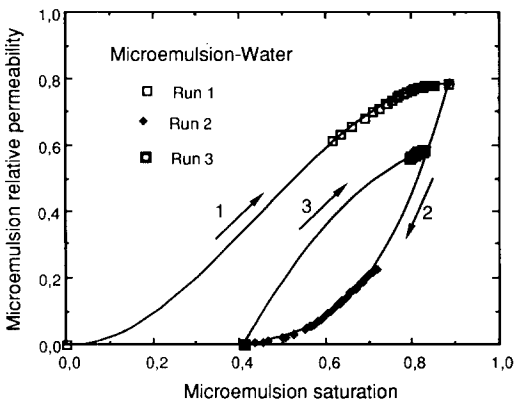

Fig. 1. Experimental two-phase relative permeabilities for microemulsion; Runs 1, 2 and 3.

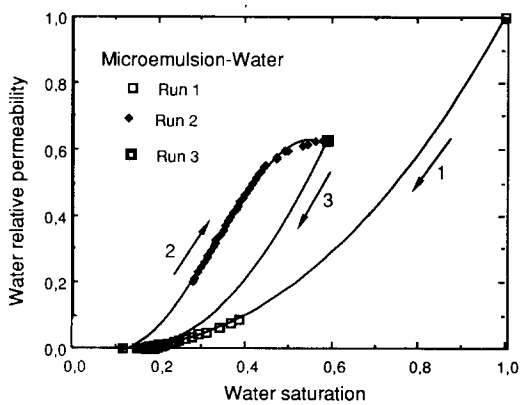

Fig. 2. Experimental two-phase relative permeabilities for water; Runs 1, 2 and 3.

discarded since there clearly is hysteresis also in the wetting phase, in Fig. 2.

Killough (1976) assumed the relative permeabilities to be reversible, until the historical maximum of the non-wetting phase saturation is reached. From Fig. 1 this is not the case; the drainage curve in Run 3 does not re-trace the inbibition curve in Run 2, and they have curvatures of opposite sign.

Microemulsion–excess oil

The core now contains microemulsion and residual excess water. Excess oil is injected in Run 4, followed by microemulsion in Run 5. From Fig. 3, the residual oil saturation is very low, with almost the same start point for Run 4 and 6, and the results for both phases are fairly close.

Hysteresis is present in the oil relative permeability and not in the microemulsion case. The lines drawn for the oil phase are from data-fitted polynomials, while only the measured data are displayed for the microemulsion phase. For Run 5, when microemulsion

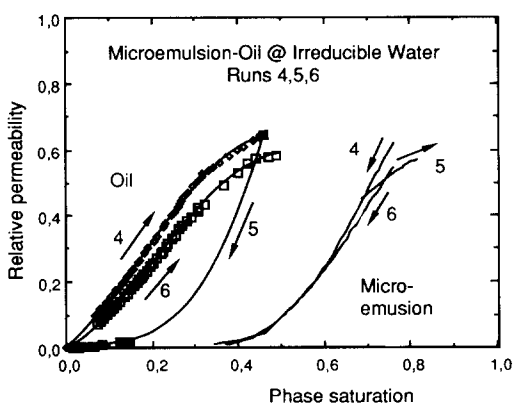

Fig. 3. Experimental two-phase relative permeabilities for oil and microemulsion; Runs 4, 5 and 6.

displaces oil, there is only a short interval of datapoints since the viscosity ratio between oil and microemulsion imposes a high breakthrough saturation.

Three-phase displacements

Of the three runs made, only Run 9 is reported in detail here, since Runs 7 and 8 exhibited limited three-phase flow. The relative permeabilities were determined by Eqs. 3a, b and c.

Core II (Table 1) was flooded with SDBS-batch II, Table 2 according to the following procedure:

(1) The core is initially saturated with 100% excess water.

(2) Microemulsion displaces excess water down to residual saturation at a rate of $q_m = 1.0$ ml/min.

(3) Excess water and oil is simultaneously injected, $q_o = q_w = 0.5$ ml/min.

Initial and end saturations are listed in Table 7, and the interpreted relative permeability

TABLE 7

Initial and end saturations for Run 9

State	S_w	S_m	S_o
Initial	0.175	0.825	0.0
End	0.331	0.334	0.335

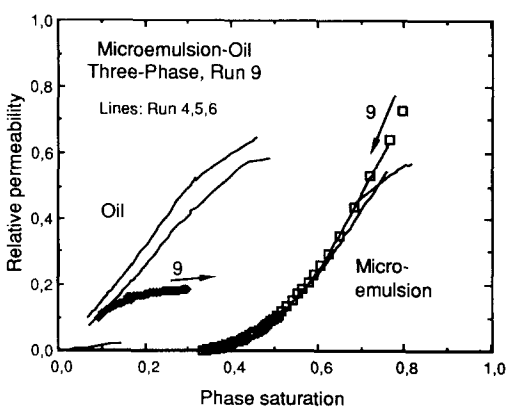

Fig. 4. Experimental relative permeability curves for excess oil and microemulsion, Run 9. Corresponding curves from Runs 4, 5 and 6 also shown.

curves for oil and microemulsion are displayed in Fig. 4. The relative permeability of the microemulsion phase does not display hysteresis, while that of the oil phase has a quite different graph than for the other runs, possibly caused by a different evolution of the water saturation.

The experiments show that drainage water relative permeabilities only depend on water saturation. The imbibition curves are quite different, and the water phase clearly exhibits hysteresis, in agreement with Skauge and Matre (1991).

Simulation

Numerical model

The simulations are performed with the chemical reservoir simulator UTCHEM (version D-3.2), Pope and Nelson (1978). The model has been continuously improved over the last years by Rogaland Research Institute. In connection with the present work, the hysteresis models of Carlson (1981) and Killough (1976) have been implemented, together with the new hysteresis model described in the Appendix. Also, an option is added for starting the simulation with three phases present.

We have validated the model by comparing input relative permeabilities with those calculated from simulated production history, by Virnovskii's (1984) method. The validation runs were performed with two and three phases flowing, limited to cases where each input relative permeability function only depends on its own saturation.

Results from the simulation showed no difference whether 40 and 80 numerical blocks were used, and all the production runs were subsequently made with 50 blocks of equal size. There was very good agreement between input and interpreted relative permeability curves, except that the interpreted curves displayed a certain amount of numerical dispersion, before frontal breakthrough.

Input data

Core dimensions and injection rates were set equal to those of the two-phase experiments.

Composition of the microemulsion phase is of no importance, since the effect of interfacial tension and changes in capillary number is not presently incorporated. The input phase behavior parameters are adjusted to produce a stable microemulsion having the same ratio of water/surfactant and oil/surfactant as in the experimental part. For simplicity, no alcohol is included in the simulations.

The two-phase experiments were used to define the relative permeability exponents ϵ_{jp}, in terms of a first or second order polynomial in saturations, and the Stone I model employed for microemulsion relative permeability.

Simulation of experiment Run 9

Relative permeabilities from the simulation are displayed in Fig. 5 as lines, together with the experimentally measured point values. The lines represent values from the last numerical block, and they are very close to those obtained by interpreting production data with Eqs. 3a, b and c.

No attempt has been made to optimize the simulation results. The simulated values follow the experiments fairly well in the microemulsion case; for water, the simulated values are shifted to higher saturations; and for oil, the experimental values are in the saturation

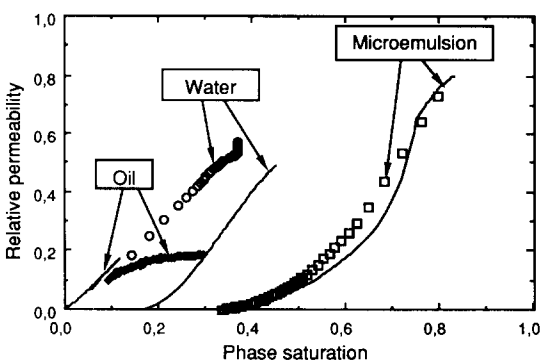

Fig. 5. Relative permeabilities from simulation and experiments; Run 9.

interval between 0.1 and 0.3, while the simulated values lie between 0.0 and 0.12.

The three-phase relative permeabilities in the model are generated from two-phase data measured on Core I. From Table 1, there is a difference between Cores I and II, on which Run 9 was conducted. In a systematic study of the validity of three-phase correlations based on two-phase hysteretic curves, the experiments should, of course, be conducted on the same core.

On close inspection, the simulated oil curve has two saturation reversals, but does not display any associated hysteresis loop. It is possible that a more pronounced hysteresis effect, achieved by changing the hysteresis parameters, would have given a better fit for both the oil and water phase.

Generally, it seems that combining two-phase measurements with the Stone I method and hysteresis effect, is a viable procedure for representing three-phase relative permeabilities.

Hysteresis

Virnovskii's theory is valid for three-phase flow, each phase relative permeability depending on two saturations. Saturation discontinuities are included in the theory, and production data can be interpreted from the start of an experiment, including intervals of single- and two-phase flow. It is not clear, however, if the theory is applicable when the relative permeabilities are hysteretic, multivalued functions of saturations. To investigate this point, we performed several simulations with varying degree of hysteretic behavior. In Fig. 6 the results of a typical run are shown. The lines represent simulated values from the outlet numerical block in the model, while the points are interpreted production data.

The match is excellent, as with all other cases we have run. Note that the hysteretic 'hook' in the water curve exhibits a multivalued relative permeability function.

In another run, hysteresis was turned off.

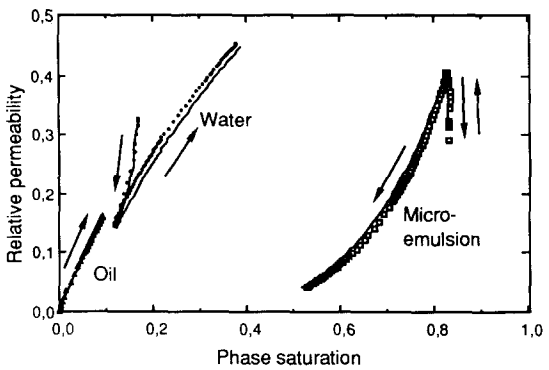

Fig. 6. Simulation results—Relative permeabilities from outlet block and from interpreted production data. Microemulsion depends on two saturations, hysteresis is incorporated.

The microemulsion phase still exhibited the same 'hook' for high saturations, caused by the fact that the microemulsion relative permeability, k_{rm}, is a function of two saturations, by the Stone I model. For interpretion of an actual laboratory experiment, it may be difficult to distinguish between a relative permeability function being influenced by hysteresis or being a function of two saturations.

When we compare water relative permeability curves at the four numerical block numbers (1, 15, 35 and 50), the 'hook' in the water curve (Fig. 6) is slightly shifted, indicating that each block, in principle, has a unique relative permeability curve when hysteresis is included. It is possible that the slight shift in the water curve for high saturation values is caused by this effect, and that Virnovskii's theory has to be modified if the saturation history varies significantly with distance along the core sample.

Discussion

Viscous instability

Pavone (1989), and Peters and Khataniar (1987) imply that the proper relative permeability curves to be used in numerical models are determined by unsteady-state measurements, also if the displacement is unstable. Skauge and Matre (1991) cannot match their displacement experiments with steady-state relative permeability curves.

Using the data in Tables 3 and 4, the Pavone number, Eq. 2, for excess water displacing microemulsion is 1.02×10^{-3}; and for excess oil displacing microemulsion 1.4×10^{-1}. The displacements are clearly unstable, and according to Peters and Khataniar (1987), the interpreted relative permeability functions will be affected.

For practical purposes, to model the flow process dependency, it seems reasonable to make the relative permeability curves depend on the stability number in addition to the capillary number. Steady-state measured relative permeability curves, it would seem, are only applicable in a direction of saturation change that has a stable displacement.

A hysteresis scheme as suggested in the Appendix, that depends on both the capillary and the stability number, could be sufficiently flexible and yet precise to model three-phase processes in general.

The density difference in our experiments (from Table 3) is about the same as in Pavone's work, where no gravity effects were observed. We therefore consider gravity effects to be negligible.

Further work

Virnovskii's theory makes it feasible to interpret three-phase displacement experiments in the same manner as the JBN-method now is used for standard two-phase displacement experiments. With three phases mobile, it is not possible to control the direction of saturation change for all three phases. A hysteresis scheme is therefore necessary as an integral part of the interpretation. It is a challenge is to design an appropriate, standardized suite of displacement experiments that uniquely will determine the parameters in the relative permeability model.

Conclusions

(1) Three-phase hysteresis effects are present in surfactant flooding.

(2) Three-phase displacement experiments are accurately interpreted by Virnovskii's theory, the relative permeabilities being functions of two saturations.

(3) The interpretation is valid from the start of the displacement, including two-phase intervals and saturation discontinuities.

(4) Virnovskii's theory also seems to be accurate when the relative permeabilities display hysteresis effects.

(5) Hysteresis in two-phase curves cannot be modelled by Killough's procedure. A scheme is developed to allow different drainage and imbibition curves at any point in the process.

(6) Two-phase hysteresis curves combined with three-phase correlations may be used to trace the experimental values.

(7) A recommended procedure should be worked out for three-phase displacement experiments to determine the parameters in the relative permeability models.

Acknowledgement

This work has been supported by SPOR—The Norwegian State R&D Program for Improved Oil Recovery and Reservoir Technology.

Appendix – Hysteresis model

We consider a three-phase system with water as the wetting phase, microemulsion the intermediate phase, and oil the non-wetting phase.

The model is inspired by the experimental results in this paper, and provides options for hysteresis loops in two-phase relative permeability curves. It is assumed that relative permeability of the microemulsion phase may be a function of two saturations, and that it may be represented by a combination of two-phase curves, e.g. Stone's (1970) model I.

The microemulsion phase is denoted by 'mw' if only water is present, and by 'mo' when oil is present at irreducible water saturation.

Two types of hysteresis are included in all four two-phase relative permeability curves: (1) two-phase, non-wetting residual saturations S_{mwr} and S_{or} are functions of their maximum historical values S_{mw}^{max} and S_{o}^{max}, and calculated by Land's (1968) method; (2) different curve shapes for saturation decrease and increase, even if the saturation reversal takes place in between the historical maximum and the associated residual saturation of the non-wetting phase.

Relative permeability curves are described by $k_r = k_{re} \cdot S_n^{\epsilon}$, with subscript 'e' denoting endpoint and 'n' normalized. To increase the flexibility, ϵ is made a function of S_n. Different ϵ-functions are used for each phase and for decrease and increase of saturation, ϵ: $\epsilon_{jp}(S_n)$, where $p \in \{D,I\}$ and 'D' denotes drainage and 'I' imbibition.

The procedure is the same for the mw- and the mo-system, except that the residual (irreducible) water saturation has to be incorporated.

Water–microemulsion

The relative permeability curve for water with the two types of hysteresis is depicted in Fig. A1, and the dual graph for microemulsion in Fig. A2. The curve numbered (1), through points ADB in Fig. A1, is for primary drainage; then imbibition (2) from B to C; and secondary drainage (3) from C to B. A straight-line interpolation from C to A is assumed to give the location of the historical maximum value of k_{rw}. The hysteresis loop DED would result from an imbibition reversal at D.

To accommodate for saturation reversals at an arbitrary point, vertical hysteresis rectangles are introduced, as exemplified for two cases in Fig. A1. A rectangle always has one corner located either on the line CA, or on the curve ADB.

For the rectangle with E in the upper right hand corner, reversal from decreasing to increasing saturation takes place at the lower point L. The upper point U (or E) cor-

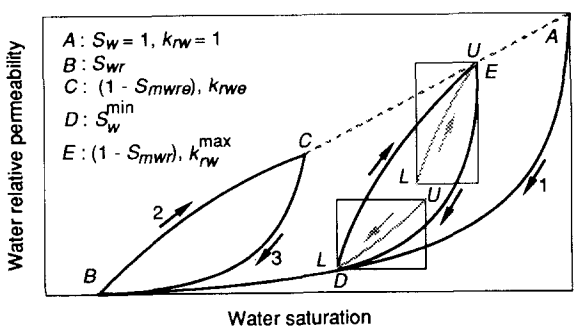

Fig. A1. Schematic of relative permeability hysteresis for water in a water–microemulsion system.

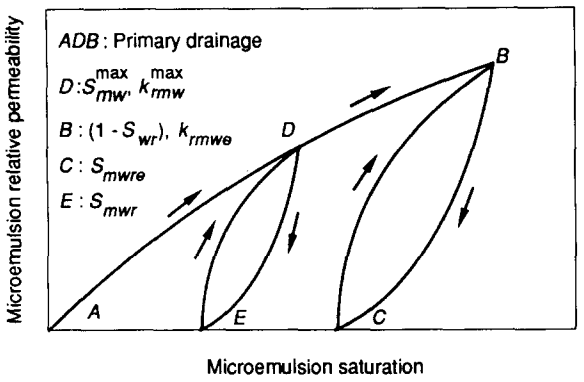

Fig. A2. Schematic of hysteresis loops for microemulsion relative permeability in a water–microemulsion system.

responds to $1-S_{mwr}$, calculated from Land's expression using a trapping constant and $S_{mw}^{max}=1-S_{w}^{min}$, the historical minimum water saturation at D. The rectangle is defined by placing U and L in opposite corners. The process proceeds from L to U along the shaded path. A new reversal may occur, or the process may continue to U, where $k_{rm}=0$.

For the lower rectangle, with D in the lower left-hand corner, the saturation reversal is at U. The lower point L (or D) is on the primary drainage curve. A rectangle is drawn with U and L in opposite corners, and a new shaded path is calculated. If no new reversal occurs, the process will reach D and proceed on the primary drainage curve DB until reversal occurs.

The relative permeability is expressed by:

$$k_{rw}=k_{rw}^{L}+(k_{rw}^{U}-k_{rw}^{L})(S_{wn}^{*})^{\epsilon_{2wp}(S_{wn})} \tag{4a}$$

where the normalized saturations are given by:

$$S_{wn}^{*}=\frac{S_w-S_w^{L}}{S_w^{U}-S_w^{L}} \tag{4b}$$

$$S_{wn}=\frac{S_w-S_{wr}}{1-S_{wr}-S_{mwr}} \tag{4c}$$

For primary drainage $S_{mwr}=0$, and otherwise calculated by Land's expression:

$$S_{mwr}=\frac{S_{mw}^{max}}{1+C_{mw}S_{mw}^{max}} \tag{5}$$

and C_{mw} is Land's trapping constant for water–microemulsion. The exponent ϵ_2 is adjusted for the fact that only a portion of the relative permeability curve is used, from S_w^{L} to S_w^{U} for the upper rectangle in Fig. A1:

$$\epsilon_{2wp}=\frac{\log\left(\dfrac{S_{wn}^{\epsilon_{wp}(S_{wn})}-(S_{wn}^{L})^{\epsilon_{wp}(S_{wn}^{L})}}{(S_{wn}^{U})^{\epsilon_{wp}(S_{wn}^{U})}-(S_{wn}^{L})^{\epsilon_{wp}(S_{wn}^{L})}}\right)}{\log(S_{wn}^{*})} \tag{6}$$

Water: drainage

On the primary drainage curve, $S_w^{L}=S_{wr}$, $k_{rw}^{L}=0$, $S_w^{U}=1$, $k_{rw}^{U}=1$.

Within the hysteresis loop DED, when $S_w>S_w^{min}$ in Fig. A1, $S_w^{L}=S_w^{min}$, $k_{rw}^{L}=k_{rw}^{min}$, and (S_w^{U}, k_{rw}^{U}) denotes the point of saturation reversal. In agreement with the hysteresis models suggested by Killough (1976) and Carlson (1981), the process follows the hysteresis branch UL until it reaches the historical minimum saturation S_w^{min}, and proceeds on the primary drainage curve.

Water: imbibition

Now $S_w^{U}=1-S_{mwr}$, and (S_w^{L}, k_{rw}^{L}) is defined as the point of saturation reversal. The maximum relative permeability value for the loop is found by linear interpolation on the line CA: $k_{rw}^{U}=1-(1-k_{rwe})S_{mwr}/S_{mwre}$. Here, S_{mwre} is residual microemulsion saturation with associated endpoint water relative permeability k_{rwe} when the start of the loop is $S_{mw}^{max}=1-S_{wr}$, and S_{mwr} is calculated from Eq. 5.

Microemulsion

The normalized saturations are given by $S_{mwn}=1-S_{wn}$, $S_{mwn}^{*}=1-S_{wn}^{*}$, and the saturation reversals at $S_{mw}^{L}=1-S_w^{U}$, $S_{mw}^{U}=1-S_w^{L}$.

Primary drainage, ADB, S_{mw} increasing: $k_{rmw}^{U}=k_{rmwe}$, the endpoint relative permeability at $(1-S_{wr})$, Fig. A2; $k_{rmw}^{L}=0$.

Secondary drainage, $S_{mw}<S_{mw}^{max}$, the maximum historical saturation, point D in the figure, $S_{mw}^{max}=(1-S_w^{min})$; $k_{rmw}^{U}=k_{rmw}^{max}$; k_{rmw}^{L} from last saturation reversal; rectangle drawn with opposite corners in points U and L, (not shown in Fig. A2).

Imbibition, (decreasing S_{mw}): $k_{rm}^{L}=0$, k_{rm}^{U} from the last saturation reversal.

Microemulsion–oil

The procedure with rectangles is the same as for microemulsion–water: oil relative permeability is determined as for microemulsion in the mw-system; and microemulsion relative permeability as for water.

In normalizing saturations, one must take into account the irreducible water saturation, $S_{iw}(=S_{wr})$:

$$S_{mon}^{*}=\frac{S_{mo}-S_{mo}^{L}}{S_{mo}^{U}-S_{mo}^{L}} \tag{7a}$$

$$S_{mon}=\frac{S_{mo}-S_{mor}}{1-S_{mor}-S_{or}-S_{wi}} \tag{7b}$$

For primary drainage $S_{or}=0$, and is otherwise calculated from Land's expression:

$$S_{or}=\frac{S_o^{max}}{1+C_{mo}S_o^{max}} \tag{8}$$

For imbibition (increasing S_{mo}), endpoint relative permeability is found by linear interpolation:

$$k_{rmo}^{U} = k_{rmow} - (k_{rmoe}^{o} - k_{rmoe})\frac{S_{or}}{S_{ore}} \quad (9)$$

where S_{ore} is the maximum value of S_{or}, i.e. the one found from Eq. 9 when $S_o^{max} = 1 - S_{iw} - S_{mor}$; k_{rmoe}^{o} is the starting value of microemulsion relative permeability, at $S_{or} = 0$, and should be equal to k_{rmwe} if $S_{iw} = S_{wr}$, which is assumed in the model.

Capillary number

Variable capillary number, and/or stability number, may be included by the following modifications:

(1) Residual saturations, S_r, exponents ϵ, and endpoint relative permeabilities k_{re} are made functions of N_{ca}.

(2) Primary drainage loop with k_{rw}^{min}, k_{rmw}^{max}, k_{rmo}^{min}, and k_{ro}^{max}, are re-calculated for each time step.

(3) The relative permeability at a saturation reversal, a corner in the hysteresis rectangle, is re-calculated for each time step.

(4) Two desaturation curves may be used, one in common for S_{wr} and S_{mor}, and another for S_{or} and S_{mwr}.

Stone's method I

The following normalizations are used:

$$S_{wn} = \frac{S_w - S_{wr}}{1 - S_{mm} - S_{wr} - S_{or}} \quad (10a)$$

$$S_{mn} = \frac{S_m - S_{mm}}{1 - S_{mm} - S_{wr} - S_{or}} \quad (10b)$$

$$S_{on} = \frac{S_o - S_{or}}{1 - S_{mm} - S_{wr} - S_{or}} \quad (10c)$$

where (Fayers and Matthews, 1984):

$$S_{mm} = \alpha S_{mwr} + (1 - \alpha) S_{mor} \quad (11)$$

and:

$$\alpha = 1 - \frac{S_o}{1 - S_{wr} - S_{mor}} \quad (12)$$

Here, S_{mor} is constant while S_{mwr} is calculated from Eq. 5. The relative permeability of the microemulsion is then:

$$k_{rm} = \frac{S_{mn}}{k_{rmwe}} \left(\frac{k_{rmw}}{1 - S_{wn}}\right)\left(\frac{k_{rmo}}{1 - S_{on}}\right) \quad (13)$$

References

Carlson, F.M., 1981. Simulation of relative permeability hysteresis to the non-wetting phase. Pap. SPE 10157, presented at the 1981 SPE Annu. Tech. Conf. and Exhib., San Antonio, Oct. 5–7.

Dria, D.E., Pope, G.A. and Sepehrnoori, K., 1990. Three-phase gas/oil/brine relative permeabilities measured under carbon dioxide flooding conditions. Pap. SPE/DOE 20184, presented at the 1990 Symp. on Enhanced Oil Recovery held in Tulsa, Okla., April 22–25.

Fayers, F.J., 1989. Extension of Stone's method 1 and conditions for real characteristics in three-phase flow. SPERE, (Nov.): 437–445.

Fayers, F.J. and Matthews, J.D., 1984. Evaluation of normalized Stone's methods for estimating three-phase relative permeabilities. SPE J., (April): 224–232.

Grader, A.S. and O'Meara, D.J., 1988. Dynamic displacement measurements of three-phase relative permeabilities using three immiscible liquids. Pap. SPE 18293, presented at the 63rd Annu. Tech. Conf. and Exhib. of the Soc. Pet. Eng., Tex., Oct. 2–5.

Huh, C., 1979. Interfacial tensions and solubilizing ability of a microemulsion phase that coexists with oil and brine. J. Colloid Interface Sci., 71: 408–426.

Johnson, E.F., Bossler, D.P. and Naumann, V.O., 1959. Calculation of relative permeability from displacement experiments. Trans. AIME, 216: 370–372.

Killough, J.E., 1976. Reservoir simulation with history-dependent saturation functions. SPE J. (Feb.): 37–48.

Kyte, J.R. and Rapoport, L.A., 1958. Linear waterflood behavior and end effects in water-wet porous media. Trans. AIME, 213: 423–426.

Lake, L.W., 1989. Enhanced Oil Recovery. Prentice Hall, Englewood Cliffs, N.J., pp. 48–58.

Land, C.S., 1968. Calculation of imbibition relative permeability for two- and three-phase flow from rock properties. SPE J. (June): 149–156; Trans. AIME, 243.

Land, C.S., 1971. Comparison of calculated with experimental imbibition relative permeability. SPE J. (Dec.): 419–425.

Maini, B.B., Kokal, S. and Jha, K., 1989. Measurements and correlations of three-phase relative permeabilities at elevated temperatures and pressures. Pap. SPE 19677, presented at the 1989 SPE Annu. Tech. Conf. and Exhib., San Antonio, Oct. 8–11.

Oak, M.J., 1990. Three-phase relative permeability of water-wet Berea. Pap. SPE/DOE 20183, presented at the 1990 Symp. on Enhanced Oil Recovery held in Tulsa, Okla., April 22–25.

Oak, M.J., Baker, L.E. and Thomas, D.C., 1990. Three-phase relative permeability of Berea sandstone. J. Pet. Technol., (Aug.): 1054–1061.

Pavone, D., 1989. Observations and correlations for immiscible viscous fingering experiments. Pap. SPE 19670, presented at the 1989 SPE Annu. Tech. Conf. and Exhib., San Antonio, Oct. 8–11.

Peters, E.J. and Khataniar, S., 1987. The effect of instability on relative permeability curves obtained by the

dynamic-displacement method. SPEFE (Dec.): 469–474.

Pope, G.A. and Nelson, R.C., 1978. A chemical flooding compositional simulator. SPE J. (Oct.): 339–354.

Quandalle, P. and Sabathier, J.C., 1989. Typical features of a multipurpose reservoir simulator. SPERE (Nov.): 475–480.

Sarem, A.M., 1966. Three-phase relative permeability measurements by unsteady-state method. SPE J. (Sept.): 199–205; Trans. AIME, 237.

Shaw, J.C., Churcher, P.L. and Hawkins, B.F., 1989. The effects of firing on Berea sandstone. Pap. SPE 18463, presented at the 1989 Int. Symp. on Oilfield Chemistry, Houston, Feb. 8–10.

Skauge, A. and Matre, B., 1991. Three-phase relative permeabilities in brine/oil/microemulsion systems. In Situ, (in press).

Stone, H.L., 1970. Probability model for estimating three-phase relative permeability. J. Pet. Technol., (Feb.): 214–218; Trans. AIME, 249.

Stone, H.L., 1973. Estimation of three-phase relative permeability and residual oil data. J. Can. Pet. Technol., 12(4): 53–61.

Virnovskii, G.A., 1984. Determination of relative permeabilities in a three-phase flow in a porous medium. (Translated from Izv. Akad. Nauk SSSR, Mekh. Zhidk. Gaza, Moscow, 5: 187–189.) ©1985 Plenum, New York.